**18th International Conference on Structural Mechanics in Reactor Technology (SMiRT 18)**
**Beijing, China, August 7-12, 2005**
**SMiRT18-H02-6**

# PREDICTION OF TRANSFER LENGTH IN PRETENSIONED PRESTRESSED CONCRETE STRUCTURES

**Byung Hwan Oh**
*Professor, Dept. of Civil Engineering, Seoul National University, Korea*
Phone: (+822)880-7350,
Fax: (+822)887-0349
E-mail: bhohcon@snu.ac.kr

**Eui Sung Kim**
*Manager of Civil Engineering Design Team, Hyundai Development Company, Korea*
Phone: (+822)880-7350,
Fax: (+822)887-0349
E-mail: eskim@hyundai-dvp.co.kr

**Young Cheol Choi**
*Research Assistant, Dept. of Civil Engineering, Seoul National University, Korea*
Phone: (+822)880-7357,
Fax: (+822)887-0349
E-mail: zerofe1@snu.ac.kr

## ABSTRACT

The purpose of the present paper is to propose a rational theory, which can evaluate the transfer lengths realistically for arbitrary designed pretensioned members. The theory considers the prestressing steel as a solid cylinder and the surrounding concrete as a hollow cylinder. The compatibility condition is then imposed at the steel-concrete interface with an appropriate equilibrium equation. The possible cracking of surrounding concrete in radial direction due to expansive pressure after prestress transfer has been considered by employing an appropriate tensile stress-crack width relation. The calculated transfer lengths were compared with the calculated ones and the comparison indicates that the theoretical prediction exhibits good correlation with test data.

**Keywords:** pretensioned prestressed concrete, transfer length, prestress transfer, strain profile

## 1. INTRODUCTION

The transfer of prestress into concrete is rather complex and important because the prestress is released to zero at the ends of these pretensioned concrete members[Hoyer (1939), Janney (1954), Laldji (1988), Marshall (1969), Oh (2000), Uijl (1995), Gopalaratnam (1985)]. One of the important features in the design of pretensioned members is the determination of correct transfer length that needs to develop prestress fully along the length of the pretensioned members[Uijl (1995), Gopalaratnam (1985)].

The current equation in the design code considers only the effects of strand diameter and prestress intensity in the calculation of transfer length in pretensioned members. However, recent study by authors[5] reports, on the basis of comprehensive experimental study, that not only the strand diameter and prestress intensity, but also the concrete strength and cover thickness affect greatly the transfer length in pretensioned members.

The purpose of the present study is, therefore, to propose a rational theoretical method which can predict the transfer length realistically for diverse pretensioned members. The proposed theory considers the prestressing steel as a solid cylinder and the surrounding concrete as a hollow cylinder. The compatibility condition is then imposed at the steel-concrete interface. The possible cracking of surrounding concrete in radial direction due to expansive pressure right after prestress transfer has been considered in the analysis by introducing an appropriate tensile

 

stress-crack width relation. The equilibrium equations are established and solved for each successive segment in longitudinal direction. The strain development curves from the end of pretensioned members were obtained from the analysis and the transfer lengths were then determined from the strain profiles along the pretensioned members.

### 1.1 Bond Mechanism

The bond stress, $\tau$ can be expressed by the following fundamental governing equation.

$$\tau = \mu p \tag{1}$$

The coefficient $\mu$ can be considered constant for a particular type of steel and combines actual frictional bond along with mechanical bond resulting from deformations projecting from the tendon surface. If the coefficient of friction is known experimentally, the bond stress can be found if the interface pressure $p$ (absolute value of radial stress) can be determined. To determine the unknown quantity $p$, a general procedure is developed here using the theory of elasticity applied to thick cylinders.

## 2. ISOTROPIC ELASTIC ANALYSIS FOR UNCRACKED CONCRETE

A idealized section for the anchorage zone of a pretensioned beam is illustrated in Fig. 1. Steel is treated as a solid cylinder and concrete as a surrounding hollow cylinder with a radial thickness equal to the smaller cover ( $c_y$ ) or the effective cover ( $c_{eff}$ ) defined by Uijl (1995). The outer surface of the notional concrete cylinder is assumed to behave as a free surface. The original radius of the steel cylinder is equal to $r_o$ (the radius of the unstressed steel). The concrete cylinder has an outer radius of and an inner radius of which is the radius of the stressed steel because the concrete is cast after the tendon is stressed first in the pretensioned members. Due to Poisson's ratio, $r_j$ is always less than $r_o$. At prestress transfer, the steel shortens and swells so a pressure develops at the interface. Using thick cylinder theory, the expressions for stresses, strains and displacements of an element can be derived by considering equilibrium and compatibility, and also imposing boundary conditions.

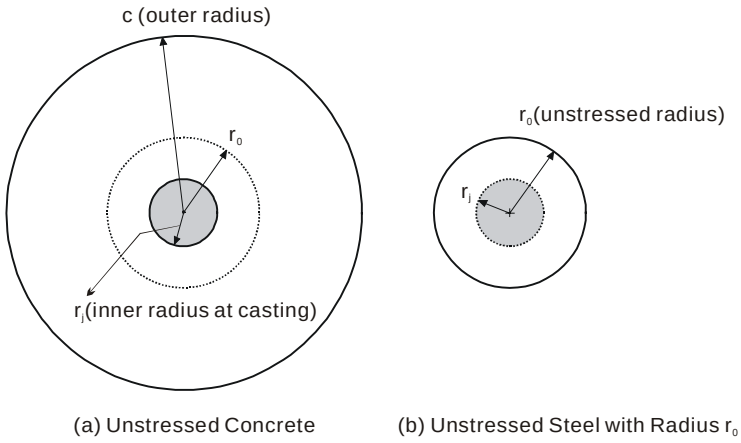


*Fig. 1 Physical dimensions of steel and concrete cylinders*

### 2.1 Equilibrium Equation

An element in the form of slice of thickness *dz* is taken at a distance z from the end to derive an equilibrium equation. The shape of the element and three-dimensional stresses acting on this element are shown in Fig. 2. Three-dimensional equilibrium of forces in the radial direction can be solved by dropping terms containing higher-order infinitesimal.

$$\sigma_r + \frac{\partial \sigma_r}{\partial r} \cdot r - \sigma_\theta + \frac{\partial \tau_{zr}}{\partial z} \cdot r = 0 \tag{2}$$

in which $\sigma_r$ = normal stress in radial direction, $\sigma_\theta$ = hoop stress in circumferential direction, and $\sigma_z$ = normal stress in axial direction, respectively.

In the longitudinal direction, all the variables are assumed to be independent of *z* direction within the small finite length *dz*. Therefore, Eq. (2) is reduced to Eq. (3).

 

$$\sigma_r + \frac{d\sigma_r}{dr} \cdot r - \sigma_\theta = 0 \tag{3}$$

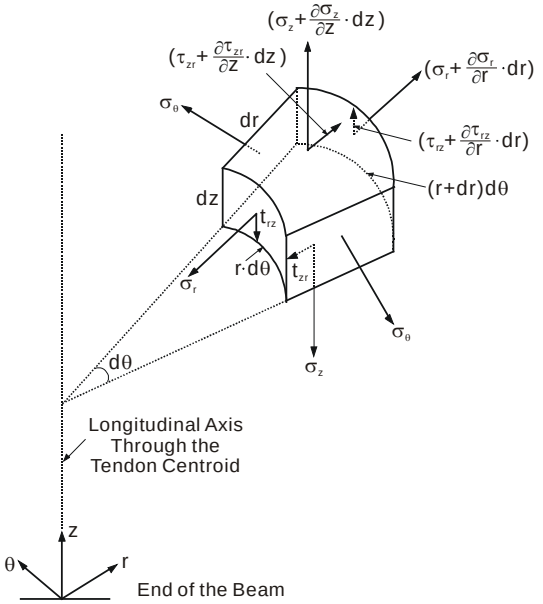


*Fig. 2 Three dimensional stresses acting on element*

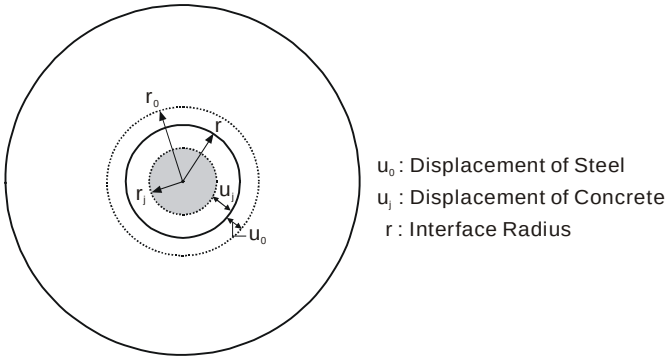


*Fig. 3 Relative radial displacement of stressed composite unit*

## 2.2 Compatibility Condition

The basic requirement to be fulfilled is the compatibility of displacements at the steel-concrete interface given by the following equation, which can be derived from Fig. 3.

$$r_o + u_o = u_j + r_j \tag{4}$$

in which $u_0$ = displacement of steel, $r_0$ = initial diameter of steel before prestressing, $u_j$ = displacement of concrete, and, $r_j$ = diameter of steel after prestressing, respectively.

## 2.3 Derivation of Radial and Circumferential Stresses

From the strain-displacement and stress-strain relations of the element, the stresses in radial and circumferential directions are expressed as Eq. (5).

$$\sigma_r = \frac{E}{1-v^2}(\varepsilon_r + v\varepsilon_\theta) + \frac{v(1+v)\sigma_z}{1-v^2} \tag{5a}$$

$$\sigma_\theta = \frac{E}{1-v^2}(\varepsilon_\theta + v\varepsilon_r) + \frac{v(1+v)\sigma_z}{1-v^2} \tag{5b}$$

Substituting Eq. (5) into Eq. (3) results in the following equidimensional equation in radial displacement.

$$r\frac{d^2u}{dr^2} + \frac{du}{dr} - \frac{u}{r} = 0 \tag{6}$$

The solution for Eq. (6) may be written as follows.

$$u = c_1 r + \frac{c_2}{r} \tag{7}$$

The radial and circumferential stresses may now be written in terms of the constants of integration, $c_1$ and $c_2$, by combining Eqs. (7) and (5).

$$\sigma_r = E\left\{\frac{c_1}{(1-v)} - \frac{c_2}{r^2(1+v)}\right\} + \frac{v\sigma_z}{(1-v)} \tag{8a}$$

 

$$\sigma_\theta = E\left\{\frac{c_1}{(1-v)} + \frac{c_2}{r^2(1+v)}\right\} + \frac{v\sigma_z}{(1-v)} \tag{8b}$$

The constants $c_1$ and $c_2$ can be determined using the boundary conditions
For the steel cylinder, the displacement at its outer surface(see Fig. 3) can be deriving by applying proper boundary conditions, i,e., $u = 0$ at $r = 0$, $\sigma_r = \sigma_\theta = f_r$ at $r = R$.

$$u_o = \left[\frac{-p(1-v_p) - v_p f_{pz}}{E_p}\right] r_o \tag{9}$$

in which $p$ = internal pressure due to steel expansion after prestress transfer, $f_{pz}$ = axial stress of prestressing steel at a distance $z$ from free end, $v_p$ and $E_p$ = Poisson's ratio and elastic modulus of prestressing steel, respectively.

For the concrete cylinder, the displacement at its inner surface(see Fig. 3) is derived by employing boundary conditions $\boldsymbol{\sigma_r = f_r}$ at $r = R$ and $\boldsymbol{\sigma_r = 0}$ at $\mathbf{r = C}$.

$$u_j = \frac{-pr_j}{E_c(1/c^2 - 1/r_j^2)}\left[\frac{(1-v_c)}{c^2} + \frac{(1+v_c)}{r_j^2}\right] - \frac{v_c f_{cz} r_j}{E_c} \tag{10}$$

in which $f_{cz}$ = axial stress of concrete at a distance $z$ from free end, $v_c$ and $E_c$ = Poisson's ratio and elastic modulus of concrete, respectively.

From the compatibility condition of Eq. (4), an expression for the interface pressure is now obtained as follows.

$$p = \frac{r_o(1 - v_p f_{pz}/E_p) - r_j(1 - v_c f_{cz}/E_c)}{(1-v_p)r_o/E_p + [v_c - (r_j^2 + c^2)/(r_j^2 - c^2)]r_j/E_c} \tag{11}$$

Finally, the radial and circumferential stresses, $\sigma_r$ and $\sigma_\theta$, can be expressed in terms of interface pressure $p$ as follows.

$$\sigma_r = \frac{-p(1/c^2 - 1/r^2)}{(1/c^2 - 1/R^2)} \tag{12a}$$

$$\sigma_\theta = \frac{-p(1/c^2 + 1/r^2)}{(1/c^2 - 1/R^2)} \tag{12b}$$

### 2.4 Demonstration of Transverse Stress Distribution

To demonstrate the stress distribution around a tendon a numerical example is considered here. For a tendon diameter $d_b = 12.7$mm, effective prestress $f_{pe} = 1{,}300$MPa, clear cover $c_y = 30$mm and concrete strength at prestress transfer $f'_{ci} = 30$MPa, the radial and circumferential stress distributions for a slice taken at the free end can be obtained from the above equations and are shown in Fig. 4.

The results of analysis shows that the tensile stress in the vicinity of tendon along the circumferential direction reaches the value approximately 10 times larger than the concrete tensile strength(Fig. 4). This means that the concrete around the tendon will experience cracking in radial direction as shown in Fig. 5. Therefore, a more refined analysis, which considers the cracking phenomenon, is required to obtain more realistic and accurate results. This will be done in the next section.

## 3. MODELING OF RADIALLY CRACKED CONCRETE AROUND TENDON

### 3.1 Nature and Modeling of Cracked Region Surrounding Steel

Fig. 5 shows the state of cracking around the prestressing steel due to expansive pressure after prestress transfer in pretensioned members. The extent of radial cracking depends on the magnitude of pressure which in turn depends on the distance from the anchorage free end.

The damage in the concrete in the radial direction can range from complete cracking to no cracking. In certain situations with small cover, the fractured zone may extend to the free surface

of the member. To represent the degree of cracking, two parameters, i.e., the reduced tensile strength ( $f_{tr}$ ) and the length of damaged zone ( $L_c$ ) are important. Three possible situations need to be considered, i.e., uncracked, partially cracked, and fully cracked cases. When a tendon is released for transfer, the concrete near the

 

end of the tendon may become fully cracked. The concrete surrounding the tendon will be only partially cracked at a certain distance from the end where the expansion pressure is not high enough. The concrete surrounding the tendon will remain intact and uncracked at a further distance from the end where the reduction of prestress in the steel is very small or negligible.

The occurrence of cracking in radial direction along the tendon yields anisotropic properties for concrete around the tendon. The stiffness of concrete in the circumferential direction is reduced according to the degree of cracking and the reduced modulus $E_\theta$ should be used for more realistic analysis

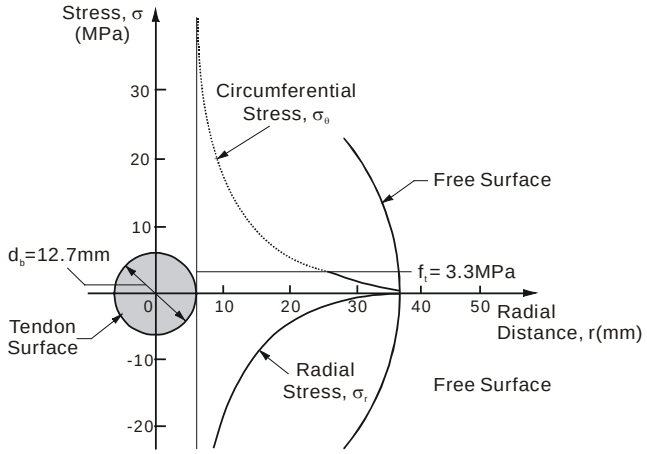


*Fig. 4 Transverse stress distributions from isotropic elastic analysis*

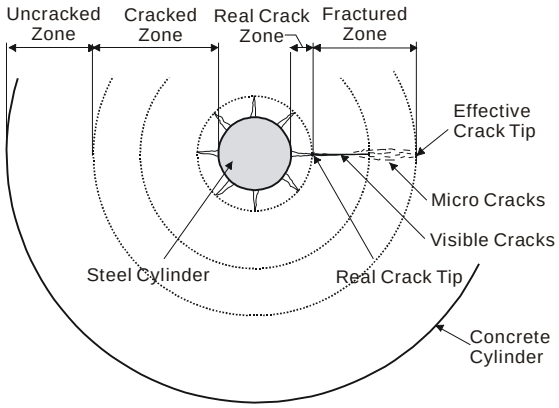


*Fig. 5 Nature of cracking around the tendon*

## 3.2 Modified Material Properties for Cracked Section

A reduced circumferential modulus of elasticity at the outer surface of cracked concrete ( $E_\theta = E_{cr}$ ) and a reduced tensile strength of concrete at the outer surface ( $f_{tr}$ ) are required for partially cracked and fully cracked analysis.

3.3.1 Determination of $E_\theta$

The strain due to $\sigma_\theta$ only maybe written as:

$$\varepsilon = \frac{\sigma_\theta}{E_c} + \frac{w}{L} = \frac{\sigma_\theta}{E_c} + \frac{wN}{2\pi r} \tag{13}$$

in which $N$ = number of radial cracks, $L = 2\pi r / N$ = crack spacing of radial cracks, and $w/L$ = average strain due to cracks.

By definition for a uniaxial condition,

$$E_\theta = \frac{\sigma_\theta}{\varepsilon} = \frac{\sigma_\theta}{\sigma_\theta / E_c + w/L} \tag{14}$$

which can be rewritten using Eq. (17) as:

$$E_\theta = \frac{\sigma_\theta}{\sigma_\theta / E_c + (m/(\sigma_\theta + h) - k)N / 2\pi r} \tag{15}$$

3.3.1 Determination of $f_{tr}$

Eq. (20) can be rearranged to determine the value of $\sigma_\theta$ as follows.

$$\left[\frac{1}{E_c} - \frac{1}{E_\theta}\right]\sigma_\theta^2 + \left[h\left(\frac{1}{E_c} - \frac{1}{E_\theta}\right) - \frac{kN}{2\pi r}\right]\sigma_\theta + \left[\frac{mN}{2\pi r} - \frac{khN}{2\pi r}\right] = 0 \tag{16}$$

or $$a_1\sigma_\theta^2 + a_2\sigma_\theta + a_3 = 0 \tag{17}$$

in which $a_1$, $a_2$, and $a_3$ are the coefficients of quadratic equation.

The solution can be expressed as

$$\sigma_\theta = \frac{-a_2 \pm \sqrt{a_2^2 - 4a_1a_3}}{2a_1} \tag{18}$$

When a crack extends to the free surface $r = c$, $E_\theta$ reaches $E_{cr}$ and the corresponding $\sigma_\theta$ becomes $f_{tr}$.

## 4. DETERMINATION OF AXIAL STRESSES AT LEVEL OF TENDON

Anisotropic analysis was implemented with due consideration of material properties for cracked concrete. From the analysis the interface pressure $p$ can be obtained.

Once the interface pressure $p$ is known, the bond stress $\tau$ can be determined for a particular $\Delta z$ increment. The change of stress in the $z$ direction, $\Delta f_{pz}$, may be computed. From the equilibrium in the longitudinal direction, $\Delta f_{pz}$ is obtained as

$$\Delta f_{pz} = \frac{\pi d_b \Delta z \tau}{A_p} \tag{19}$$

Therefore, the value of steel stress at section $i+1$ is

$$\left(f_{pz}\right)_{i+1} = \left(f_{pz}\right)_i + \Delta f_{pz} \tag{20}$$

Prestressing force at section $i+1$ is then obtained as

$$P_{i+1} = \sum_{i=1}^{n} \left[\left(f_{pz}\right)_{i+1} A_p\right] \tag{21}$$

The stress in the concrete at the level of the tendon under consideration is

$$\left(f_{cz}\right)_{i+1} = P_{i+1}\left[\frac{1}{A} + \frac{e_y}{I} y\right] \tag{22}$$

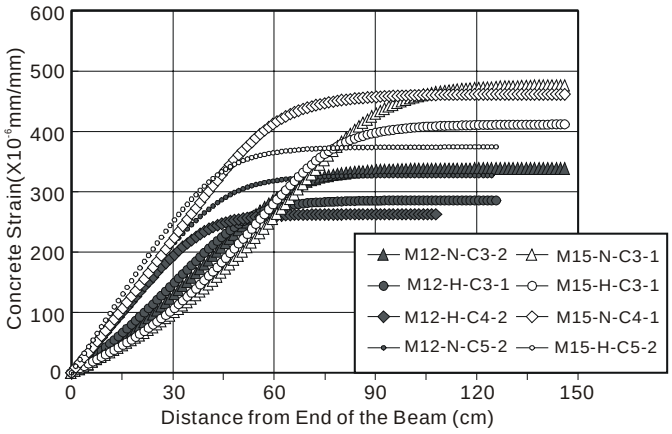


*Fig. 6 Typical theoretical prestress build-up curves*

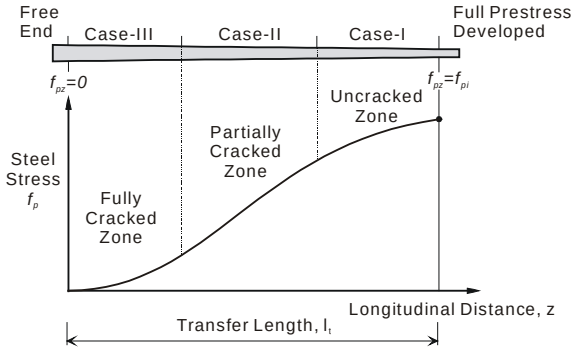


*Fig. 7 Stress build-up in the transfer zone*

## 5. CONSTRUCTION OF PRESTRESS BUILD-UP CURVES IN CONCRETE

The step-by-step analysis can be carried out for increments of $\Delta z$ from the free end until the steel stress reaches the effective prestress, $f_{pe}$, where the bond stress $\tau \cong 0$. Then the theoretical prestress build-up curves due to transfer of prestress force in pretensioned members can be constructed as shown in Fig. 6. Fig. 7 shows the schematic diagram for the prestress development in concrete due to the transfer of prestress force of prestressing steel.

## 6. COMPARISON OF THEORETICAL RESULTS WITH TEST DATA

In order to show the validity of proposed theoretical analysis, theoretical results were compared with the test data of authors' experimental program. The major test variables include the number and nominal diameter of prestressing strands, concrete compressive strength, bottom cover, and spacing of prestressing strands

The theoretical transfer lengths are computed based on the measured concrete strength at transfer, initial prestress level, cover thickness and strand diameter. The determination of transfer length was based on the concept

 

of average maximum strain method proposed recently by Oh (2000). The theoretical and experimental strain distribution curves for the typical two cases are compared in Fig. 8 and Fig. 9. General shapes of strain development curves are very much similar between measured and calculated values. It is thought that some difference between measured and calculated concrete surface strains is mainly due to the short-term creep and shrinkage effects in the first 5 to 6 hours after release during the measurements of surface strains of concrete. However, this does not cause any problem in determining the transfer length as can be seen in Fig. 8 – 9.

For specimens with mono strand, theoretical and experimental transfer lengths are compared in Fig. 10 according to strand size. The cut end in Fig. 10 represents the end of the test beam where the prestressing strands are cut directly for prestress transfer, while the dead end is the opposite end. Fig. 10 indicates that the theoretical transfer lengths correlate very well with test data and are in between those of cut and dead ends.

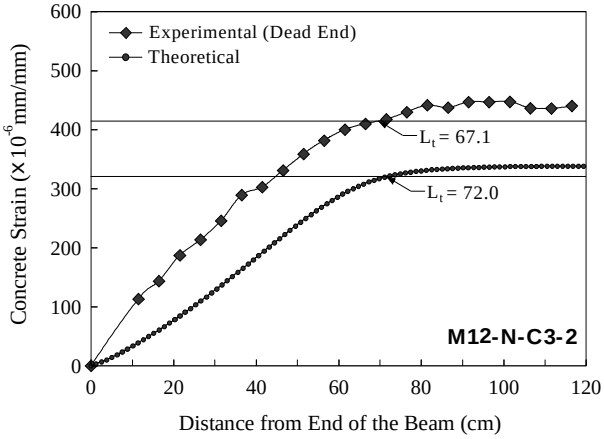


*Fig. 8 Comparison of theoretical and experimental strain build-up curves for specimen M12-N-C3-2*

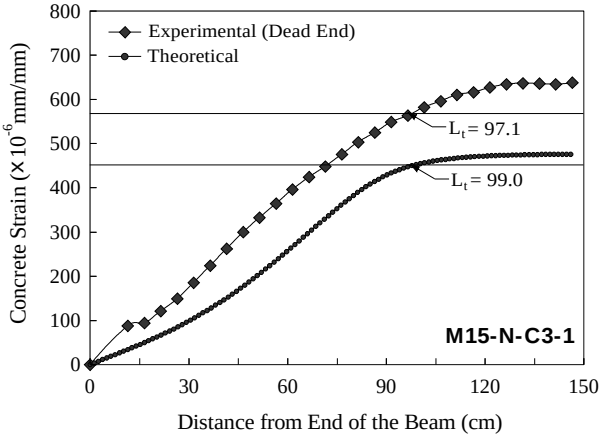


*Fig. 9 Comparison of theoretical and experimental strain build-up curves for specimen M15-N-C3-1*

## 7. CONCLUSIONS

The current design equation considers only the prestress intensity and strand diameter to calculate the transfer length of prestressing steels. However, other important parameters such as concrete strength and concrete cover may also influence the transfer length significantly. The purpose of the present study is, therefore, to propose a rational method which can calculate the transfer length realistically.

The theory proposed here considers the prestressing steel as a solid cylinder and the surrounding concrete as a hollow cylinder. The compatibility condition is then imposed at the steel-concrete interface, together with the equilibrium equation that must be satisfied in the members.

 

The radial expansion of prestressing steel due to prestress transfer may cause cracking of surrounding concrete in radial direction depending upon the magnitude of stress. The present study takes into account the effects of partial and full cracking due to expansive pressure in constructing the governing equation. The reduction of elastic modulus and tensile strength of damaged concrete due to cracking has been taken care of by employing an appropriate tensile stress stress-crack width relation.

The equilibrium equations are solved for each successive segment of a member in the longitudinal direction and the strain development curves from the ends of pretensioned concrete members are generated. The transfer lengths of pretensioned members were then determined from these strain development profiles.

The comparison of theoretical results with present test data shows good agreement. The proposed method enables to predict realistically the transfer lengths of pretensioned prestressed concrete members with various design variables.

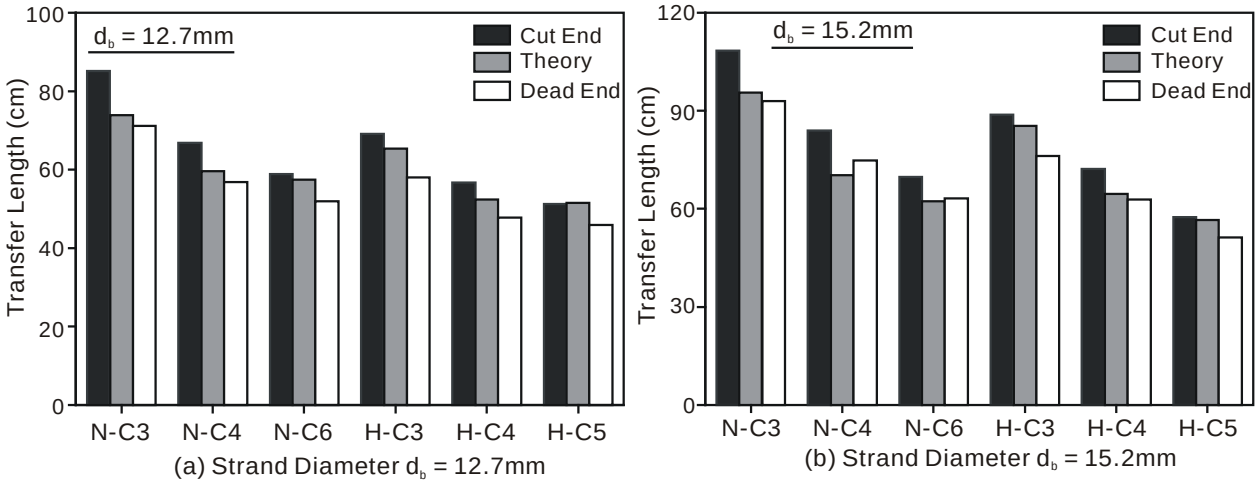


*Fig. 15 Comparison of theoretical and experimental transfer length for mono strand test series*

## REFERENCES


Hoyer, E., and Friedrich, E., (1939), *Beton und Eisen*, V. 30, No. 6, pp. 107-110.

Janney, J. R., (1954), ACI Journal, Vol. 50, No. 9, pp. 717–736.

Laldji, S., and Young A. G., (1988), Magazine of Concrete Research, Vol. 40, No. 143, pp. 90-98.

Marshall, W. T., and Krishnamurthy, O., (1969), The Indian Concrete Journal, Vol. 43, pp. 244–253 and 257.

Oh, B. H. and Kim, E. S., (2000), ACI Structural Journal, Vol. 97, No. 6, pp. 821-830.

Uijl, J. A. den, (1995), Progress in Concrete Research, Vol. 4, pp. 75-90.

Gopalaratnam, V. S., and Shah, S. P., (1985), ACI Journal, Vol. 82, No. 3, pp. 310–323.


## ACKNOWLEDGEMENTS


The support from NRL (National Research Laboratory) Program of Korea is greatly appreciated.